Korean J. Chem. Eng., 33(6), 1813-1822 (2016)
DOI: 10.1007/s11814-016-0052-3

pISSN: 0256-1115
eISSN: 1975-7220

Influence of polymeric additives on paraffin wax crystallization in model oils

Taesung Jung, Jong-Nam Kim, and Seong-Pil Kang†

Climate Change Research Division, Korea Institute of Energy Research, 152 Gajeong-ro, Yuseong-gu, Daejeon 34129, Korea
(*Received 26 October 2015 • accepted 18 February 2016*)

Abstract−Wax deposition, precipitation, and gelation make the transport of crude oil in pipelines challenging. The effect of several ethylene copolymers, and small molecules with a long alkyl chain, on wax formation was investigated for n-$C_{32}H_{66}$ in decane and de-aromatized white oil. Addition of a small amount of EVA (ethylene-*co*-vinyl acetate) copolymers delayed nucleation by reducing the onset temperature and the wax appearance temperature. They modified the wax crystal-structure and morphology from large plates to tiny particles by adsorbing to the wax surfaces and inhibiting growth. Viscosity and the pour-point were improved by inhibiting the formation of large aggregates. It was demonstrated that the content of vinyl acetate groups in EVA copolymers affected wax crystallization. The small molecules, propylene copolymers, and ethylene copolymers with ethyl acrylate, maleic anhydride, and ethylene glycol showed a weak inhibiting effect. The effect of wax inhibitors was determined by the content and by the type of structure-disturbing groups in the copolymers.

Keywords: Wax, Crystallization, Inhibitors, Nucleation, Crystal Modification, Viscosity

INTRODUCTION

Wax deposition, precipitation, and gelation in pipelines cause many problems during production and transport of crude oil. Typically, waxes are solids made up of long-chain, normal or branched alkanes with 16-50 or more carbon atoms in the chain [1]. Normal alkanes (n-paraffins) are predominantly responsible for pipeline wax deposition and gelation, which results in blocking of the oil flow, when they are cooled below the wax appearance temperature (WAT) or the pour-point [1-3]. The WAT or the onset temperature (T_{onset}) is the temperature at which wax nucleation and crystal growth start. The properties represent crystallization event during wax formation. The wax crystals formed can agglomerate and entangle at the pour-point by making gel-network and increasing viscosity. Typically, wax precipitation strongly depends on the chemical components of crude oil and on environmental factors such as temperature, cooling rate, and flow rate.

There are several ways to control wax formation downhole and in oil pipelines [1-3]. Mechanical methods (e.g., periodic pigging or cutting) and thermal methods (e.g., insulation and heating of flow lines) have been applied to prevent wax deposition [4]. Chemical methods such as inhibitors, dispersants, and diluents are also useful for preventing wax deposition and removing existing deposits [4,5]. Most of the thermal and chemical methods are related to a shift in the saturation line of the wax crystallization by increasing the temperature or decreasing the wax concentration. However, these control methods incur capital costs for heating pipelines or operational costs for huge amounts of diluents.

Wax inhibitors can provide practical, economic means for managing wax deposition because only small amounts are needed and have a large effect. Polymeric wax inhibitors are widely applied in pipeline transportation of waxy crude oils to alleviate wax deposition and may also be used as pour-point depressants or flow improvers for waxy crude oils [3,6]. Ethylene copolymers with small alkene, maleic anhydride, and acrylonitrile groups have been proposed as deposition inhibitors [1,3,7-9]. EVA (ethylene-*co*-vinyl acetate) copolymers and comb polymers can be efficient wax crystal inhibitors [1]. Before applying wax inhibitors in oilfields, their performance and effectiveness on wax inhibition should be considered for model oil systems using proper screening methods. Differential scanning calorimetry has been used to characterize nucleation of wax and the effect of wax inhibitors [10,11]. Optical microscopy and x-ray scattering methods are useful in microscopic visualization of crystallization and determination of crystal structure [12,13]. Investigation of the pour-point, yield stress, and viscosity has provided insight into the flow behavior of waxy crude oil [14,15].

We used several ethylene copolymers with vinyl acetate, ethylene glycol, ethyl acrylate, and maleic anhydride groups, a propylene copolymer, and small molecules with a long alkyl chain, which can act as kinetic inhibitors, to control the crystallization of a model waxy oil in decane and de-aromatized white oil. The influence of these kinetic inhibitors on wax formation was determined by differential scanning calorimetry, optical microscopy, and rheometer techniques, focused on nucleation, wax crystal growth, and flow behavior.

EXPERIMENTAL

1. Materials

Decane (C10, anhydrous, 99%) solvent and n-alkane wax, dotri-

†To whom correspondence should be addressed.
E-mail: spkang@kier.re.kr
‡This article is dedicated to Prof. Huen Lee on the occasion of his retirement from KAIST.

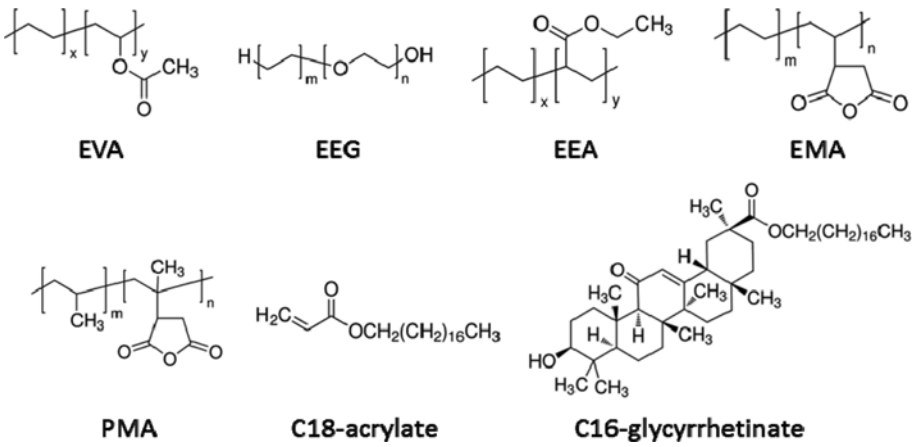

Fig. 1. Structure of additives: Copolymers and small molecules with a long alkyl chain.

acontane (n-$C_{32}H_{66}$, C32, 97%) were purchased from Alfa Aesar without further purification. The white oil solvent, Exxsol D80 (b.p. 208 °C, density 0.795 g/ml at 15.6 °C, viscosity 2.18 mm²/s at 25.0 °C), which is de-aromatized (aromatic content 0.2 wt%) hydrocarbon fluid, was obtained from ExxonMobil and used as received. Three poly(ethylene-*co*-vinyl acetate) copolymers, EVA12, EVA25, and EVA40 were used as additives (the numbers mean the vinyl acetate content: 12, 25, and 40 wt%, respectively). Three ethylene copolymers: polyethylene-*block*-polyethylene glycol (EEG, 20 wt% ethylene glycol), poly(ethylene-*co*-ethyl acrylate) (EEA, 18 wt% ethyl acrylate), polyethylene-*graft*-maleic anhydride (EMA, 0.5 wt% maleic anhydride) and one propylene copolymer: polypropylene-*graft*-maleic anhydride (PMA, 8-10 wt% maleic anhydride), were used as wax additives. To compare the inhibiting ability against wax formation of copolymers and small molecules with a long alkyl chain, octadecyl acrylate (C18-acrylate) and stearyl glycyrrhetinate (C16-glycyrrhetinate) were also used. All the copolymers and small molecules with long alkyl chains were provided by Aldrich and used as received. The structures of the additives are represented in Fig. 1.

Additive stock solutions containing 1 wt% of the copolymers and small molecules were prepared by dissolving them in decane or D80, respectively. C32 stock solutions were also prepared by dissolving C32 in decane or D80 and heating to 70 °C (above the melting temperature of C32) for 10 min. By mixing the additive stock solutions and C32 stock solutions, model waxy oil samples of 4 wt% C32, with and without 0.5 wt% additives, were prepared. Prior to analysis, the samples of the mixtures were heated to 70 °C and held for 10 min to remove the memory effect of the wax crystals.

2. Methods

2-1. Differential Scanning Calorimetry

Differential scanning calorimetry (DSC) analyses were performed with a Perkin Elmer DSC 4000. After the model waxy oil was heated to 70 °C to dissolve the wax completely, about 5 mg of model waxy oil was placed in a DSC sample pan (20 μL) and hermetically sealed to avoid vaporization of the solvent. After the sample was transferred to the DSC cell, it was melted at 70 °C for 10 min. The model waxy oil was first cooled to −20 °C at a cooling rate of 10 °C/min. After being kept at this temperature for 10 min, it was heated to 70 °C at a heating rate of 10 °C/min. Since nucleation is affected by the operation environment, a different cooling rate was chosen in this study to investigate its effect on wax formation, assuming different cooling conditions in pipelines during the transportation of crude oil. After being held at 70 °C long enough to remove the memory effect, it was finally cooled to −20 °C at a cooling rate of 5 °C/min. Herein, the temperatures, 70 and −20 °C were selected to ensure complete dissolution and crystallization, respectively of 4 wt% C32 wax. The onset temperature (T_{onset}), which corresponds to the temperature at which nucleation occurs, was indicated by deviation of the heat flow from the baseline, and was calculated using Pyris software.

2-2. X-ray Diffraction and Optical Microscopy

To make waxy gel, 5 mL of the model waxy oil with decane was cooled in a vial from 70 to 0 °C at a cooling rate of 10 °C/min. A 10 μL aliquot of waxy gel solution was transferred to a glass substrate and observed using an optical microscope (Olympus, BX-51). The waxy gel aliquot was covered with a glass cover slip and its morphology was analyzed. The remaining waxy gel in the vial was filtered and solid precipitates were dried in a vacuum oven at room temperature. The solid precipitates were ground to powder and their structures were characterized using powder X-ray diffraction (XRD, Rigaku, D/MAX-2500) from 3 to 60° using Cu Kα radiation with a 0.02° step width.

For the model waxy oil in decane with EVA copolymers, real-time microscopic visualization of crystallization events was assessed using an optical microscope coupled with a digital camera, a hot stage (Linkam, THMS600), and a temperature controller (Linkam, T95) that could precisely control the sample temperature from −196 to 600 °C at a maximum heating rate of 150 °C/min and a maximum cooling rate of −100 °C/min with liquid nitrogen. The sample was first heated to 70 °C and then cooled to 0 °C at a cooling rate of 5 °C/min. The images were recorded every 12 s during cooling. The WAT was measured, which corresponds to the temperature where wax crystallites first appeared in the microscope images.

2-3. Rheometry

The rheological behavior of the model waxy oils comprising 4 wt% of C32 in C10, or D80 with EVA40 copolymer, was characterized with a rheometer (AR2000ex, TA Instruments) equipped with a stainless-steel cone and plate system (60 mm in diameter,

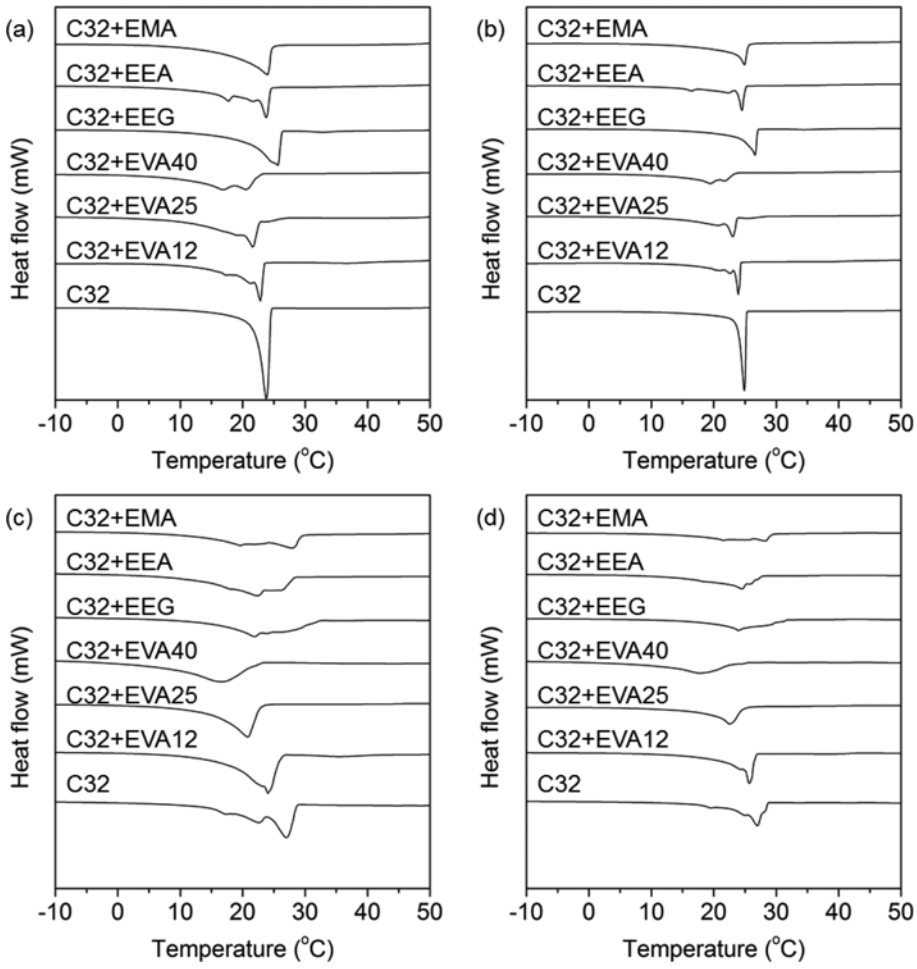

Fig. 2. DSC curves of 4 wt% C32 in (a), (b) C10 and (c), (d) D80, with and without 0.5 wt% additives at cooling rates of (a), (c) 10 and (b), (d) 5 °C/min.

cone angle of 2°). Temperature control was achieved in the standard configuration via a Peltier plate system. Prior to transfer of the sample to the Peltier plate, the plate was heated to 70 °C and then cooled to 60 °C after 5 min. A temperature-ramp experiment was performed in the range of 60 to 0 °C at a cooling rate of 1 °C/min, at three different shear rates (1, 10, 100 s^{-1}). The slow ramp rate was chosen to minimize the thermal lag effect. The viscosity data were recorded at intervals of 15 s, and the gel point was simply selected as that where the viscosity increased quickly.

Another temperature-ramp experiment was carried out to determine the pour-point where the solid-like behavior of a complex fluid takes predominance over its liquid-like behavior. As wax molecules precipitate out, the solid-like behavior increases and is manifested in the form of a sharp increase in the magnitude of the loss modulus [12]. The pour-point is the temperature at which the loss modulus (G′) becomes higher than the storage modulus (G″), hence G′>G″. At the pour-point, tan δ is '1', which is defined as the ratio of the loss modulus to the storage modulus. In our experiments, the loss modulus and the storage modulus were measured by imposing a low-amplitude (0.1 Pa) oscillatory shear stress at a frequency of 0.2 Hz and delay time of 10 s, while the sample was cooled from 60 to 10 °C at a cooling rate of 1 °C/min.

RESULTS AND DISCUSSION

1. Nucleation

DSC cooling curves for 4 wt% C32 in decane or D80 fluids, with and without 0.5 wt% ethylene copolymers, are shown in Fig. 2. The temperature at which the heat flow changed during cooling represents the onset temperature (T_{onset}) of crystallization. T_{onset}

Table 1. T_{onset} for crystallization of 4 wt% C32 in C10 and D80, with and without 0.5 wt% additives at cooling rates of 10 and 5 °C/min

	10 °C/min		5 °C/min	
	C10	D80	C10	D80
None	24.5	28.7	25.2	28.2
EVA12	23.5	26.2	24.2	26.6
EVA25	22.7	22.9	23.7	24.6
EVA40	22.5	22.1	23.4	23.3
EEG	26.2	32.4	27.0	30.6
EEA	24.4	28.5	25.0	27.9
EMA	25.6	29.0	24.9	29.2

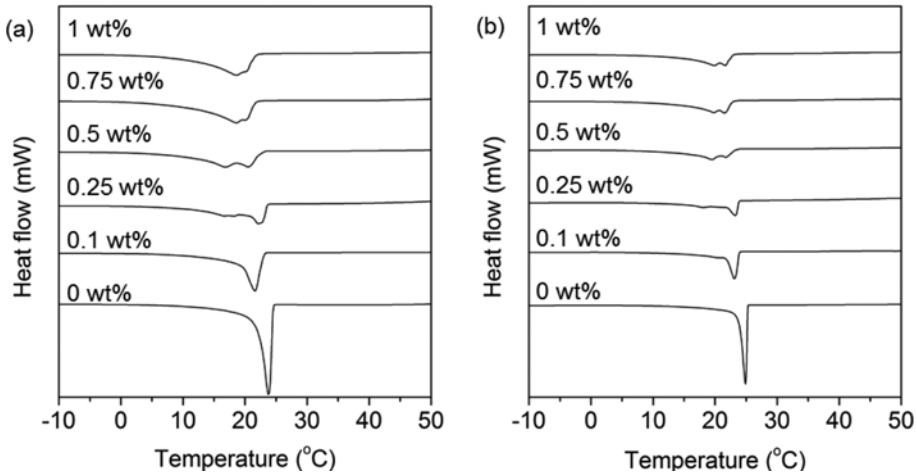

Fig. 3. DSC curves of 4 wt% C32 in C10, with and without 0.1-1 wt% EVA40 at cooling rates of (a) 10 and (b) 5 °C/min.

in relation to various additives is summarized in Table 1. For the model waxy oils in C10, at a cooling rate of 10 °C/min, T_{onset} decreased on addition of 0.5 wt% EVA12 copolymers (Fig. 2(a)). Moreover, T_{onset} further decreased when EVA25 or EVA40 was used, demonstrating the effect of the content of vinyl acetate in the polymer chains, on nucleation of the C32 wax crystals. Although the copolymers have ethylene groups that can act as templates for heterogeneous nucleation, it is thought that crystal nucleus formation is inhibited or delayed owing to vinyl acetate groups that have structures different from those of the alkyl chains in n-paraffin wax. When the content of vinyl acetate in EVA copolymers was increased, the DSC peak was broadened, shifted to lower temperatures, and with slightly less area (ΔH was not considered because of small differences between samples). These results suggest that crystallization was depressed, and occurred at lower temperatures, by addition of EVA copolymers.

Compared with EVA copolymers, EMA slightly reduced T_{onset}, because the content of maleic anhydride in EMA used in this study was only 0.5 wt% although the molecular size of the maleic anhydride group is comparable to that of the vinyl acetate group in EVA copolymers. EEG in this study had 20 wt% ethylene glycol groups but showed less effect on the decrease in T_{onset} than did the EVA copolymers. It is remarkable that T_{onset} was increased by addition of EEG. This may be related to the structural similarity between the ethylene group in paraffin wax and the ethylene glycol group in EEG. However, EEA reduced T_{onset} more than EEG and EMA in some cases, because it has 18 wt% of large ethyl acrylate groups. Taken together, both the content and the size of the structure-disturbing groups in the copolymer chains are important factors in selection of crystallization inhibitors.

The inhibiting effect of EVA copolymers on nucleation was also observed at the slower cooling rate of 5 °C/min (Fig. 2(b)). It was found that that T_{onset} at 5 °C/min was higher than T_{onset} at 10 °C/min. To induce spontaneous nucleation, the solution should be subcooled below solubility to reach a high degree of supersaturation. The difference between the subcooling temperature and the solubility is termed as the metastable zone width (MSZW). In general, the MSZW kinetically depends on the operation environment such as the cooling rate during crystallization and the slower cooling rate results in a narrower MSZW [16]. It is also notable that the peak area at 5 °C/min is smaller than that at 10 °C/min because of the narrow MSZW. As in the cases described above, other ethylene copolymers showed similar results for the reduction of T_{onset} at the cooling rate of 5 °C/min.

It was noticed that the de-aromatized D80 white oil resulted in higher T_{onset} than C10 (Fig. 2(c) and (d)). The broader peaks resulted from the complexity of the solvent molecules and the difference in the solubility of C32 in them because D80 was composed of a mixture of n-alkanes (C11 to C14), isoalkanes, and cyclic hydrocarbons. EVA copolymers showed an inhibiting effect on nucleation of C32 in D80, despite the fact that their effect was less than in C10. As described in C10, EEA was more effective for reduction of T_{onset} than were EMA and EEG in D80.

Fig. 3 and Table 2 show that T_{onset} and the peak shape strongly depend on the concentration of EVA40 in C10 at both cooling rates. It was demonstrated that a very small amount (0.1 to 0.25 wt%) of EVA40 was an effective kinetic inhibitor. Therefore, the copolymers are better than conventional wax dissolvers such as toluene, xylenes, and limonene, when considering the amount of additive needed and its cost [1]. The ethylene copolymers used in this study can give high-performance inhibition of wax-nuclei formation using only a small amount of additive (≤1 wt%).

2. Structural Modification

The powder x-ray diffraction pattern of the C32 paraffin wax

Table 2. T_{onset} for crystallization of 4 wt% C32 in C10 with 0.1 to 1 wt% EVA40 at cooling rates of 10 and 5 °C/min

wt%	10 °C/min	5 °C/min
0	24.5	25.2
0.1	23.6	23.9
0.25	23.0	23.8
0.5	22.5	23.4
0.75	21.7	22.8
1	21.5	22.6

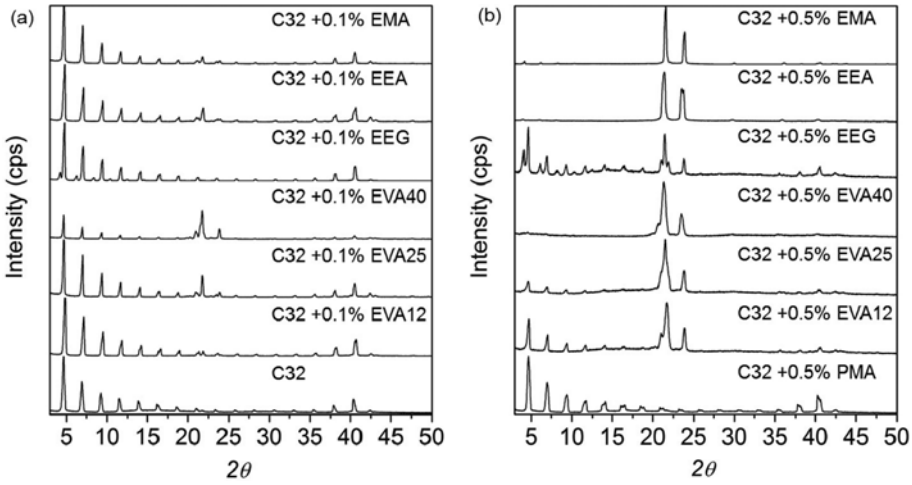

Fig. 4. X-ray diffraction patterns of the solid precipitates filtered from the mixtures of 4 wt% C32 and C10, with and without (a) 0.1 wt% and (b) 0.5 wt% additives upon cooling from 70 to 0 °C at a rate of 10 °C/min.

crystals that were precipitated without additive by fast cooling showed periodic peaks from low to mid angles (Fig. 4(a)). It is known that even-numbered n-paraffins with C>26 usually have monoclinic, orthorhombic, and rotator phases [13,17]. The orthorhombic structure phase can be induced by slow cooling, and the rotator phase appears just below the melting point of wax. In our experiment, it was intended to induce the monoclinic structure by fast cooling. The XRD pattern represents lamellar ordering of crystals on (00*l*) plane, where *l* is an integer (≥3) from 4.6°. When 0.5 wt% EVA copolymers were added (Fig. 4(b)), the intensity of the low-angle peaks decreased, but high-angle peaks emerged around 21 and 24°. The intensity ratio of high-angle peaks to low-angle peaks increased when the vinyl acetate content in the EVA copolymers was increased from 12 to 40 wt%. Similar behavior has been reported for poly(ethylene-butene) and poly(maleic anhydride amide-*co*-α-olefin) [13,18]. The decrease in low-angle peaks is ascribed to the

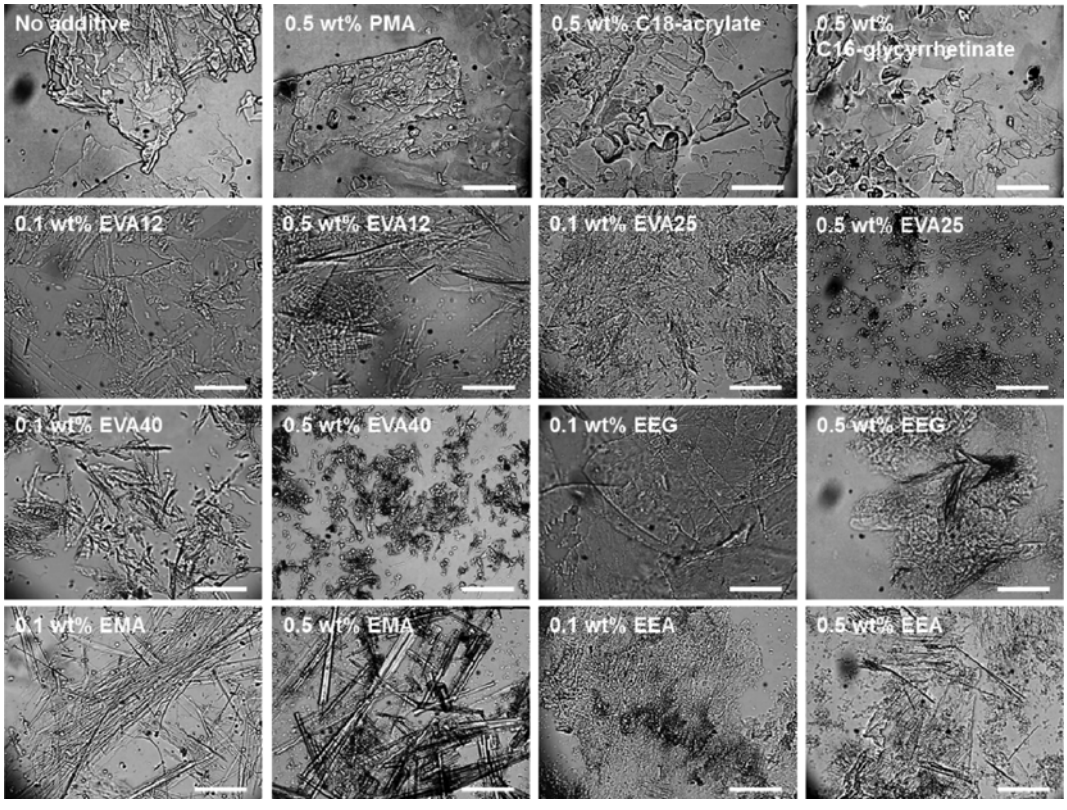

Fig. 5. Optical microscope images of the model waxy gels from 4 wt% C32 and C10, with and without 0.1, 0.5 wt% additives upon cooling from 70 to 0 °C, at a rate of 10 °C/min. Scale bars represent 100 μm.

breakage of the lamellar ordering of crystals, and the increase in high-angle peaks is attributed to the development of (110) and (200) reflections of the monoclinic structure [19] by addition of the EVA copolymers. This implies that the EVA copolymers can change the structure of C32 crystals by acting on the crystal planes. Similar to the actions of modifiers used in bio-mineralization [20], the alkyl chain of EVA copolymers can attach to the methylene group of (110) or (200) planes, thereby inhibiting the growth of the planes or disrupting the lamellar structure.

Addition of 0.5 wt% EEA and 0.5 wt% EMA also showed a distinct change from low-angle peaks to high-angle peaks. Addition of 0.5 wt% EEG did not increase high-angle peaks and showed a doublet, probably by orthorhombic structure. The reason is not clear yet. The difference in the inhibiting effect between EEA and EEG is attributed to the aforementioned difference in molecular structures of their polymer chains. Unlike the ethylene glycol groups in EEG, the ethyl acrylate groups in EEA significantly hinder the formation of the lamellar structure of C32 crystals because of their structural difference from the ethylene groups in n-paraffin wax. PMA copolymer with propylene groups did not change the XRD patterns. Furthermore, small molecules with a long alkyl chain (C18-acrylate and C16-glycyrrhetinate) also did not affect the low-angle and high-angle peaks of C32 wax crystals (data are not shown). Therefore, it may be concluded that the presence of ethylene groups in additives is necessary for adsorption onto wax crystal faces, and that the ethylene group should be large to cover the wax crystal lattice.

When the concentration of the additives was 0.1 wt%, the intensity of high-angle peaks decreased, but the effect was more distinguishable (Fig. 4(a)). Since the increase in high-angle peaks is attributed to the change of the C32 crystal structure, the effect of copolymer additives increased in the order EEG<EMA~EVA12<EEA<EVA25<EVA40. It is interesting that the change effect of wax crystal structure by the additives is similar to their inhibitory effect on nucleation as shown in Fig. 2. It may be thought that the structure change of wax crystals is closely related to the structure of the copolymer additives.

3. Morphological Modification

As shown in Fig. 5, C32 precipitates within n-paraffin wax, have a thin plate-like morphology with a large (001) face. The side faces of the monoclinic crystals are composed of (010), (110), and (100) [21]. When 0.5 wt% of EVA12, EVA25, and EVA40 copolymers were added, the habit of crystals was changed to long needles and tiny particles, respectively. The morphological change is closely related to the size reduction of the (001) face. The surface (001) consists mainly of the methyl groups at the end of alkane molecules, while surface (010), (101) and (111) comprises mainly the methylene groups of alkane molecules [22]. The ethylene groups in EVA copolymers have affinity to the methylene groups and therefore adsorb to the (010), (101) and (111) faces. This results in the inhibition of crystal growth on the side faces and reduction of the (001) face. Similar behaviors were reported for wax crystallization in the presence of poly(octadecyl acrylate), poly(ethylene-butene), and poly(maleic anhydride amide-*co*-α-olefin) [8,11,21,23-25]. The content of vinyl acetate affected the growth inhibition ability of EVA copolymers (as mentioned above) for inhibited nucleation and structural modification. A smaller (0.1 wt%) addition of EVA12 and EVA25 copolymers was less effective in morphological modification. However, EVA40, which showed the strongest effect on nucleation inhibition and structure modification, produced needle-like crystals with 0.1 wt% of addition.

The other ethylene copolymers, EEG, EMA, and EEA produced plate-like, stick-like, and needle-like C32 crystals with 0.1 to 0.5 wt% of addition. This suggests that their inhibiting effect increased in the order EEG<EMA<EEA but was weaker than the EVA copolymers. Good agreement was observed among the inhibition strengths of nucleation, and both structural and morphological modifications. The small molecules with C18 or C16 alkyl groups did not change the morphology at all. This is because they did not hinder crystal growth or block growth sites whether they were incorporated into the crystal faces or not.

The crystal growth event for 4 wt% C32 in C10, with and without EVA40, was monitored using an optical microscope with a temperature-controlled hot stage. Upon cooling at 5 °C/min, plate-

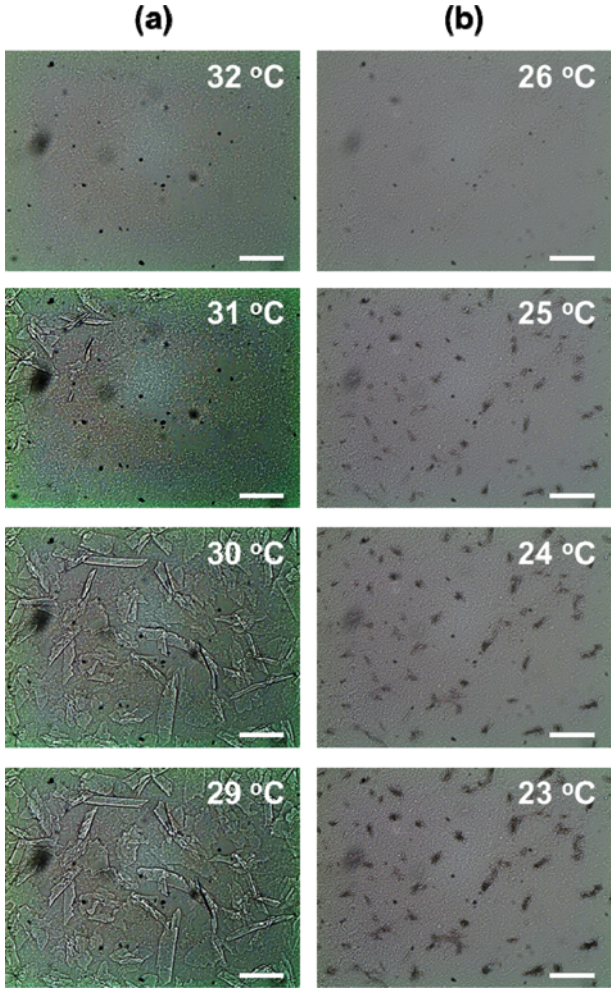

Fig. 6. Real-time monitoring of wax crystallization events for the mixtures of 4 wt% C32 and C10 (a) without and (b) with 0.5 wt% EVA40. Optical microscope images were taken upon cooling from 70 to 0 °C at a rate of 5 °C/min. Scale bars represent 100 μm.

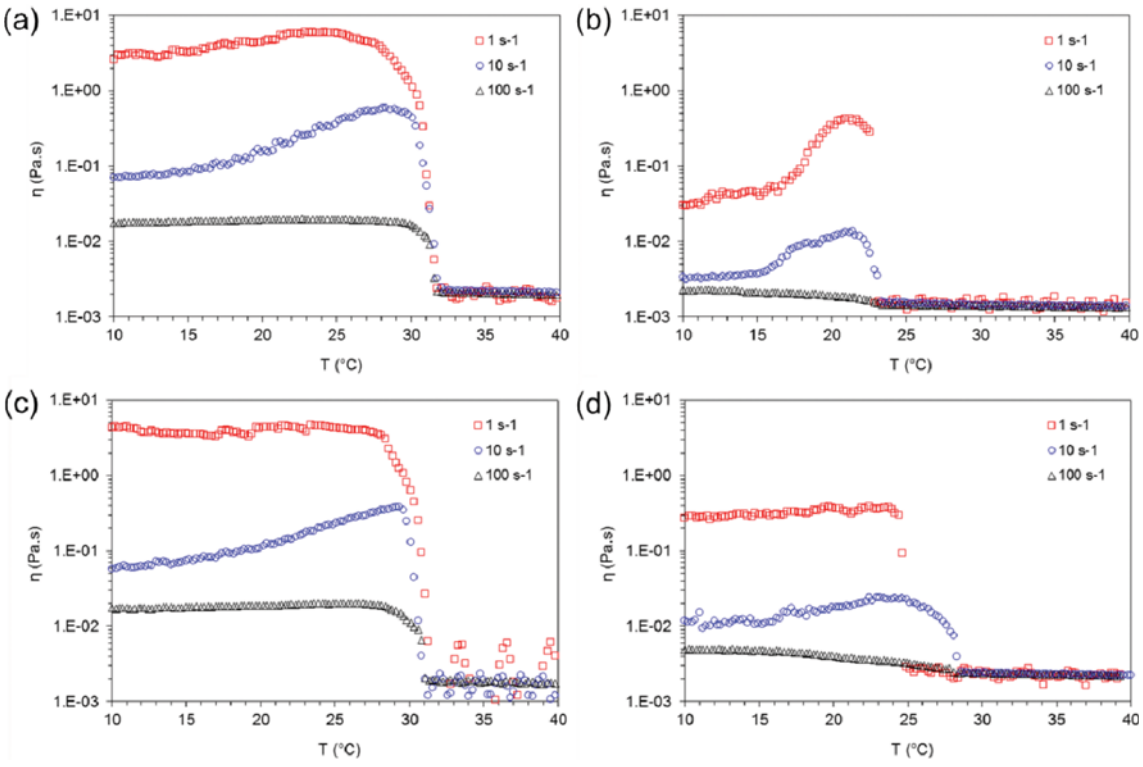

Fig. 7. Viscosity change during cooling of model waxy gels from 4 wt% C32 in (a), (b) C10 or (c), (d) D80 at shear rates of 1 (squares), 10 (circles), and 100 (triangles) s^{-1}. The concentrations of EVA40 were (a), (c) '0', and (b), (d) 0.5 wt%.

like crystals were observed at 31 °C, in the absence of additive (Fig. 6(a)). The temperature at which wax crystals appear is defined as the WAT. The WATs were about 30 and 27 °C for 0.5 wt% EVA12 and EVA25, respectively (images not shown). The WAT further decreased to 25 °C when 0.5 wt% EVA40 was added to the model waxy oil (Fig. 6(b)). The difference in T_{onset} and the WAT probably originated from the environment of the system, which can affect the kinetics of crystallization. It is notable that the crystals were dramatically changed to tiny particles, and that their size was not significantly increased during further cooling to 0 °C. The reduction of the WAT by addition of EVA40 agrees well with its inhibition effect on nucleation. Moreover, the morphological change observed using real-time microscopic visualization accords with the modification observed in the aforementioned macroscopic crystallization.

4. Flow Behavior

Fig. 7 shows viscosity as a function of temperature for 4 wt% 32 waxy oil, with and without 0.5 wt% EVA40, in C10 and D80 solvents. The shear rates chosen were 1, 10, and 100 s^{-1}. These are within the typical shear-rate range found in oil pipelines (about 20 s^{-1}). For the model waxy oil in C10 without EVA40, the viscosity slowly increased at temperature above 32 °C, showing Newto-

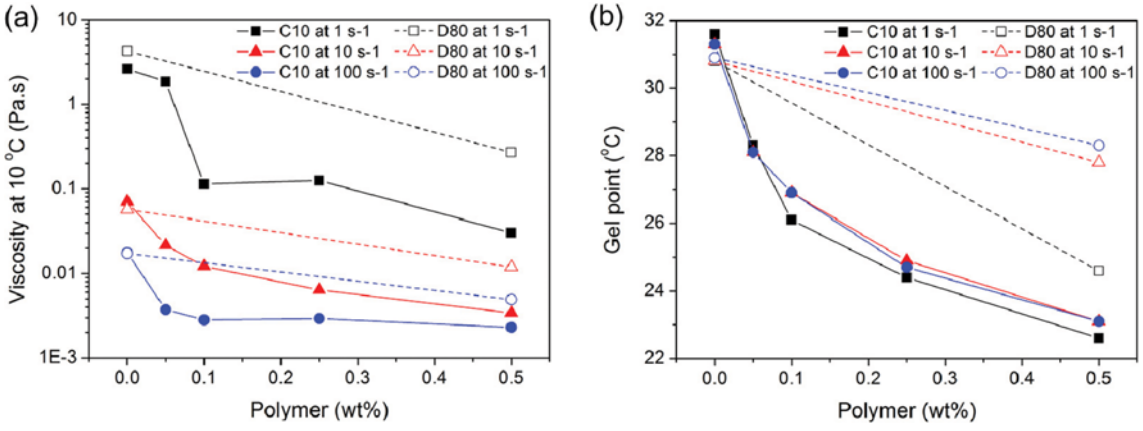

Fig. 8. Effect of EVA40 concentration in the mixture of 4 wt% C32 with C10 or D80 on (a) the viscosity at 10 °C, and (b) the gel point.

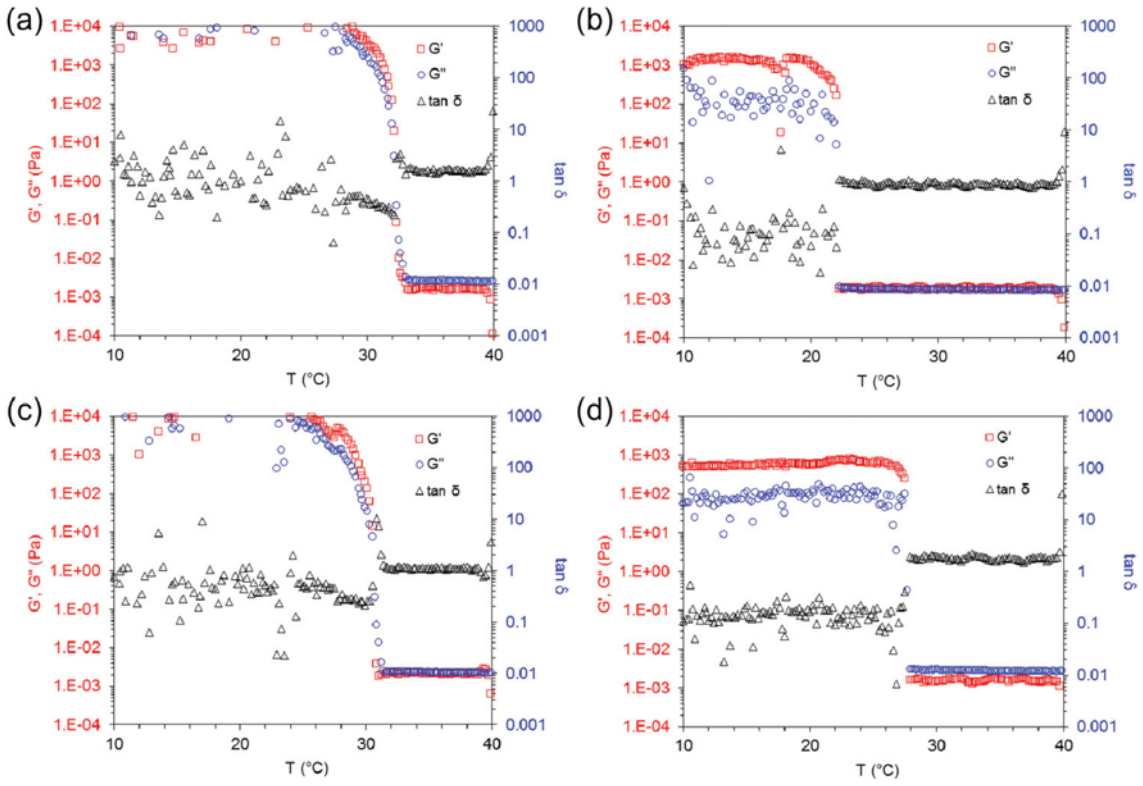

Fig. 9. Loss modulus (G′, squares), storage modulus (G″, circles) and tan δ (triangles) during cooling of model waxy gels from 4 wt% C32 in (a)-(d) C10 or (e), (f) D80 with or without EVA40. The concentrations of EVA40 were (a), (c) '0', and (b), (d) 0.5 wt%.

nian behavior. The reduction of viscosity by addition of inhibitors has been similarly reported for copolymers [15,26,27]. When the temperature was around 31 °C, the apparent viscosity dramatically increased. The gel point temperature is defined as that at which a waxy gel is formed. Regardless of shear rates (from 1 to 100 s^{-1}), the gel points values were similar (Fig. 8(b)). However, the viscosity of the model waxy gel decreased with increasing shear rate (Figs. 7 and 8(a)). When 0.05 wt% EVA40 was added to the model waxy gel in C10, the gel point dropped to 28 °C. With increase in the amount of EVA40 added (to 0.5 wt%), the gel point further decreased to about 23 °C. D80 fluids showed slightly lower gel points than did C10 without EVA40. However, the decrease in the gel point by EVA40 was small for D80. The decrease in viscosity by EVA40 also was reduced for D80. The reduced effect of EVA40 in D80 may be related to complexity in the composition of D80 fluids, but more detailed investigation is needed.

EVA40 copolymer showed an inhibiting effect on nucleation as well as on morphological and structural modifications of C32 wax crystals. As mentioned earlier, EVA40 lowered T_{onset} and the WAT, meaning wax crystallization was inhibited. Note that EVA40 reduced crystal size remarkably by adsorption to wax crystal surfaces. In general, large plate-like wax crystals formed in oil can be aggregated by packing and deposited onto the interior surface of the pipeline. However, from the decrease in viscosity and the gel point, it is inferred that they did not make large aggregates or a waxy gel network. It is rather thought that the above-mentioned tiny wax particles produced by adding EVA40 did not stick together. EVA40 copolymer has vinyl acetate groups with a different molecular structure from the alkyl groups in wax. When EVA40 is incorporated into the wax surface, the vinyl acetate groups may be exposed on the outer surface of wax particles. Therefore, they can act as surfactants or dispersants for wax particles and inhibit the formation of large aggregates. Copolymers forming tiny stabilized wax particles can alleviate flow-assurance problems, although wax crystals are inevitably formed in oil pipelines [28].

In Fig. 9, the loss modulus (G′) and the storage modulus (G″) as a function of temperature, are shown for 4 wt% C32 in C10 and

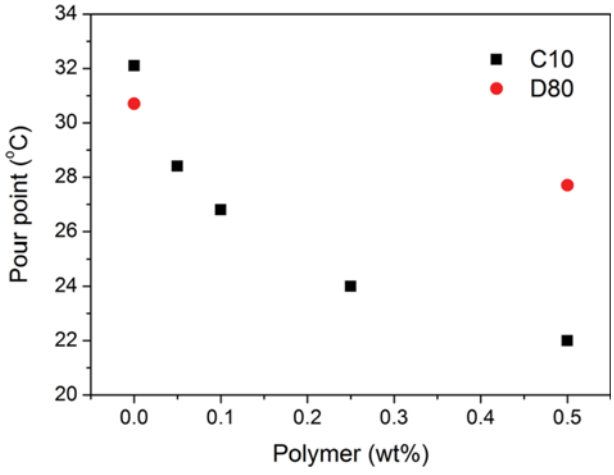

Fig. 10. Effect of EVA40 concentration in the mixture of 4 wt% C32 with C10 or D80, on the pour-point.

D80, with and without 0.5 wt% EVA40. For the wax in C10, G″ is larger than G′ and tan δ is larger than '1' above 32 °C (meaning the liquid-like behavior is dominant). When the temperature was lowered, a steep increase in G″ and G′ was found [14,29]. At the pour-point (~32 °C), G″ became smaller than G′ and solid-like behavior was dominant for the model waxy oil. By addition of EVA40 to the oil, it was found that the pour-point decreased. With increase EVA40, the pour-point decreased to 22 °C for 0.5 wt% of dosage (Fig. 10). Likewise, it has been reported that the pour-point and the relative yield-stress decreased with the concentration of effective flow improvers [6,7,18,30,31].

For both solvents, C10 and D80, the pour-points are in a good agreement with the gel points. These values are slightly higher than the T_{onset} revealed by DSC analyses, probably because of the difference in the environment or the fluidity of samples. The pour-point from D80 was slightly lower than that from C10, for the oil without EVA40. When 0.5 wt% EVA40 was added, the pour-point for D80 was higher than that for C10, meaning that the inhibiting effect of EVA40 on the pour-point could be lessened. The effects of several copolymers on nucleation, structural/morphological modifications, and flow behavior were investigated for model waxy oil by various methods. Further studies are needed for development of characterization methods for opaque oil. More complex systems with various components that could represent crude oil more realistically also need to be evaluated for potential application of copolymer wax inhibitors in oil-field operations.

CONCLUSIONS

The effect of ethylene copolymers and small molecules with a long alkyl chain was studied using DSC, optical microscopy, XRD, and rheometry. Adding small amounts of EVA copolymers and EEA lowered T_{onset} and changed the DSC peak shape for the C32 model waxy oil system in both C10 and D80 solvents, suggesting delayed nucleation. EVA and EEA copolymers disrupt the lamellar structure of the wax formed in C10 without additive, possibly by adsorbing to the wax crystal surfaces and thereby inhibiting their growth. By ex situ and in situ optical microscopy, these additives changed the morphology of the wax crystals from large plates to tiny particles and decreased the WAT. It is notable that the increasing content of vinyl acetate groups in the EVA polymer chains affected nucleation, structure, and morphology of the C32 wax crystals.

Compared with EVA and EEA, EMA with 0.5 wt% maleic anhydride content, and EEG with ethylene glycol groups, were less effective for inhibition, concluding that both the content and the size of the structure-disturbing groups in copolymer chains are important factors in the selection of crystallization inhibitors. It was demonstrated that small molecules (C16 to C18 alkyl chains) did not affect crystallization, suggesting that the alkyl chains should be large enough to cover the crystal face, in order to hinder the growth of wax crystals. With increased amount of EVA40, T_{onset}, the gel point, and the pour-point were reduced, as revealed by DSC and rheometry. The ethylene copolymer was effective, even by addition of less than 1 wt%. This additive reduced viscosity, the gel point, and the pour-point by making tiny wax particles and by inhibiting the formation of large aggregates. Wax crystallization inhibitors such as ethylene copolymers are promising for controlling wax deposition and thereby improving oil flow in pipelines.

ACKNOWLEDGEMENT

This work was supported by the Industrial Strategic Technology Development Program (No. 10045068, Development of flow assurance and organic acid/calcium removal process for the production of offshore opportunity crude) funded by the Ministry of Trade, Industry & Energy (MI, Korea). We also acknowledge Miss Ju-Young Shin for her DSC experiments and Dr. Wook-Hyun Lee for his kind support.

REFERENCES

1. M. A. Kelland, *Production chemicals for the oil and gas industry*, CRC Press, Boca Raton, FL (2014).
2. J. Becker, *Crude oil waxes, emulsions, and asphaltenes*, Pennwell Books, Tulsa, OK (1997).
3. F. Yang, Y. Zhao, J. Sjöblom, C. Li and K. G. Paso, *J. Dispersion Sci. Technol.*, **36**, 213 (2015).
4. D. W. Jennings and K. Weispfennig, *Energy Fuels*, **20**, 2457 (2006).
5. B. F. Towler and S. Rebbapragada, *J. Petrol. Sci. Eng.*, **45**, 11 (2004).
6. L. V. Castro and F. Vazquez, *Energy Fuels*, **22**, 4006 (2008).
7. L. Li, J. Xu, J. Tinsley, D. H. Adamson, B. A. Pethica, J. S. Huang, R. K. Prud'homme and X. Guo, *AIChE J.*, **58**, 2254 (2012).
8. X. Guo, B. A. Pethica, J. S. Huang, D. H. Adamson and R. K. Prud'homme, *Energy Fuels*, **20**, 250 (2006).
9. A. Aiyejina, D. P. Chakrabarti, A. Pilgrim and M. Sastry, *Int. J. Multiphase Flow*, **37**, 671 (2011).
10. X. Guo, B. A. Pethica, J. S. Huang and R. K. Prud'Homme, *Macromolecules*, **37**, 5638 (2004).
11. J. Xu, S. Xing, H. Qian, S. Chen, X. Wei, R. Zhang, L. Li and X. Guo, *Fuel*, **103**, 600 (2013).
12. R. Venkatesan, J.-A. Östlund, H. Chawla, P. Wattana, M. Nydén and H. S. Fogler, *Energy Fuels*, **17**, 1630 (2003).
13. L. Li, X. Guo, D. H. Adamson, B. A. Pethica, J. S. Huang and R. K. Prud'homme, *Ind. Eng. Chem. Res.*, **50**, 316 (2011).
14. S. Chen, G. Øye and J. Sjöblom, *J. Dispersion Sci. Technol.*, **28**, 1020 (2007).
15. K. Cao, X.-x. Wei, B.-j. Li, J.-s. Zhang and Z. Yao, *Energy Fuels*, **27**, 640 (2013).
16. W. Beckmann, *Crystallization: Basic concepts and industrial applications*, Wiley, Weinheim (2013).
17. E. Marie, Y. Chevalier, F. Eydoux, L. Germanaud and P. Flores, *J. Colloid Interface Sci.*, **290**, 406 (2005).
18. H. Jiang, J. Xu, X. Wei, T. Wang, W. Wang, L. Li and X. Guo, *J. Appl. Polym. Sci.*, **131** (2014).
19. P. Shashikanth and P. Prasad, *Indian J. Eng. Mater. Sci.*, **7**, 225 (2000).
20. K. Sangwal, *Additives and crystallization processes: From fundamentals to applications*, Wiley, Chichester (2007).
21. D. M. Duffy and P. M. Rodger, *Phys. Chem. Chem. Phys.*, **2**, 4804 (2000).
22. C. Wu, J.-l. Zhang, W. Li and N. Wu, *Fuel*, **84**, 2039 (2005).
23. X. Guo, B. A. Pethica, J. S. Huang, R. K. Prud'homme, D. H.

Adamson and L. J. Fetters, *Energy Fuels*, **18**, 930 (2004).
24. A. Radulescu, D. Schwahn, J. Stellbrink, E. Kentzinger, M. Heiderich, D. Richter and L. J. Fetters, *Macromolecules*, **39**, 6142 (2006).
25. J. Xu, H. Qian, S. Xing, L. Li and X. Guo, *Energy Fuels*, **25**, 573 (2011).
26. K. S. Pedersen and H. P. Rønningsen, *Energy Fuels*, **17**, 321 (2003).
27. T. Wang, J. Xu, M. Wang, X. Wei, M. Shen, J. Huang, R. Zhang, L. Li and X. Guo, *J. Appl. Polym. Sci.*, **132** (2015).
28. H. P. Soni and D. Bharambe, *Energy Fuels*, **22**, 3930 (2008).
29. F. Yang, C. Li and D. Wang, *Energy Fuels*, **27**, 1307 (2013).
30. A. L. Machado and E. F. Lucas, *Pet. Sci. Technol.*, **19**, 197 (2001).
31. H. S. Ashbaugh, X. Guo, D. Schwahn, R. K. Prud'homme, D. Richter and L. J. Fetters, *Energy Fuels*, **19**, 138 (2005).